Cerebral Cortex, January 2017;27: 602–615

doi:10.1093/cercor/bhv255
Advance Access Publication Date: 26 October 2015
Original Article

ORIGINAL ARTICLE

Reduced Hemispheric Asymmetry of Brain Anatomical Networks Is Linked to Schizophrenia: A Connectome Study

Yu Sun[1], Yu Chen[1], Simon L. Collinson[2], Anastasios Bezerianos[1] and Kang Sim[3,4]

[1]Singapore Institute for Neurotechnology (SINAPSE), Centre for Life Sciences, [2]Department of Psychology, National University of Singapore, Singapore, [3]Department of General Psychiatry and [4]Department of Research, Institute of Mental Health (IMH), Singapore

Address correspondence to Dr Yu Sun, Singapore Institute for Neurotechnology (SINAPSE), Centre for Life Sciences, National University of Singapore, Singapore 117456. Email: lsisu@nus.edu.sg

Downloaded from https://academic.oup.com/cercor/article/27/1/602/3056183 by guest on 11 October 2020

Abstract

Despite convergent evidence indicating a variety of regional abnormalities of hemispheric asymmetry in schizophrenia, patterns of wider neural network asymmetry remain to be determined. In this study, we investigated alterations in hemispheric white matter topology in schizophrenia and their association with clinical manifestations of the illness. Weighted hemispheric brain anatomical networks were constructed for each of 116 right-handed patients with schizophrenia and 66 matched healthy participants. Graph theoretical approaches were then employed to estimate the hemispheric topological properties. We found that although small-world properties were preserved in the hemispheric network, a significant hemispheric-independent deficit of global integration was found in schizophrenia. Furthermore, a significant group-by-hemisphere interaction was revealed in the characteristic path length and global efficiency, attributing to significantly reduced hemispheric asymmetry of global integration in patients compared with healthy controls. Specifically, we found reduced asymmetric nodal efficiency in several frontal regions and the hippocampus. Finally, the abnormal hemispheric asymmetry of brain anatomical network topology was associated with clinical features (duration of illness and psychotic psychopathology) in patients. Our findings provide new insights into lateralized nature of hemispheric dysconnectivity and highlight the potential for using brain network measures of hemispheric asymmetry as neural biomarkers for schizophrenia and its clinical features.

Key words: diffusion tensor imaging, graph theory, hemispheric asymmetry, schizophrenia, structural connectivity

Introduction

Hemispheric structural asymmetry of the brain has been well documented in adults and children (Geschwind and Levitsky 1968; Galaburda et al. 1978; Toga and Thompson 2003), and shows a degree correspondence with hemispheric specialization of function, with the left hemisphere regarded as being specialized for language as well as handed preference and the right hemisphere as being dominant for some nonverbal functions, including spatial attention and processing of faces (Toga and Thompson 2003; Herve et al. 2013). Traditionally, research regarding structural asymmetries in the brain has focused on macroscopic gray matter (GM) asymmetries. Among the most prominent observation of brain asymmetry is the so-called Yakovlevian torque (i.e., the right frontal and left occipital petalias) in the development of asymmetry (Toga and Thompson 2003). Furthermore, brain volumetric and cortical thickness

© The Author 2015. Published by Oxford University Press. All rights reserved. For Permissions, please e-mail: journals.permissions@oup.com

asymmetries have been demonstrated in focal regions, which show varying degrees of correspondence to brain functions (Good et al. 2001; Watkins et al. 2001; Lancaster et al. 2003). For instance, leftward volume asymmetries have been consistently observed in the inferior frontal gyrus (Broca's area) and the superior temporal gyrus (Wernicke's area), which are considered as an anatomical marker of left hemispheric functional specialization for language processing (Geschwind and Levitsky 1968). Evidence from recent studies has shown that structural asymmetry not only exhibits in GM, but also in white matter (WM) that interconnects cortical brain regions (Cao et al. 2003; Takao, Abe, et al. 2011). For instance, using diffusion tensor imaging (DTI, an in vivo imaging method for probing WM microstructure and connectivity), studies have repeatedly reported a leftward asymmetry of the arcuate fasciculus and the anterior cingulum in healthy individuals (Gong et al. 2005; Parker et al. 2005; Vernooij et al. 2007; Glasser and Rilling 2008; Takao, Hayashi, et al. 2011; Song et al. 2014), which provide an additional anatomical insight into lateralized cognitive abilities.

Atypical lateralization in brain structure is associated with aging (Cabeza 2002) and several neuropsychiatric disorders (Crow et al. 1989; Kubicki et al. 2003; Park et al. 2004; Wang et al. 2004; Takao et al. 2010; Oertel-Knochel and Linden 2011). Among these psychiatric disorders, schizophrenia has been repeatedly shown to be associated with abnormal hemispheric asymmetry in both postmortem (Crow et al. 1989; Falkai et al. 1995; Highley et al. 1999) and neuroimaging investigations (Luchins et al. 1982; Bilder et al. 1994; DeLisi et al. 1997; Collinson et al. 2003; Kubicki et al. 2011; Mueller et al. 2015), which may represent a derailment in processes that establish normal hemispheric specialization of cognitive functions, for example, impaired speech processing has been proposed as a key cognitive factor in the manifestation of schizophrenia symptoms (Heinrichs and Zakzanis 1998; Mesholam-Gately et al. 2009). The prevalence of nonright-handedness has also been reported to be significantly higher in patients with schizophrenia than in healthy individuals (Sommer et al. 2001), which may also indicate a failure to establish cerebral asymmetry. The search for causes of disrupted lateralization in schizophrenia is ongoing and inconclusive (Shenton et al. 2001; Ribolsi et al. 2014). One influential theory was proposed by Crow, who has suggested that schizophrenia stems from a failure of normal hemispheric lateralization in temporal lobe brain regions that are important for language production (Mitchell and Crow 2005), and that this failure is genetically determined (Crow 2008). In fact, over the last 30 years, a large body of evidence has supported the presence of abnormalities in temporal lobe morphology. It has been suggested that temporal lobe abnormalities are key to understanding schizophrenia due to the interconnected nature of temporal neural networks that subserve language and memory (Shenton et al. 1992; McCarley et al. 1999). More recently, a research interest in WM fiber tracts subserving anatomical connections between distinct brain regions and its lateralized manifestation in schizophrenia is emerging (Kubicki et al. 2007), coinciding with the recent advent of structural DTI technique. Convergent evidence has shown a reduced leftward asymmetry in particular WM tracts, including the anterior cingulum (Park et al. 2004; Wang et al. 2004), the uncinate fasciculus (Kubicki et al. 2002; Ribolsi et al. 2009; Miyata et al. 2012), the inferior occipito-frontal fasciculi (Miyata et al. 2012), and the superior occipito-frontal fasciculi (Kunimatsu et al. 2008; Carletti et al. 2012). In one recent meta-analysis of DTI studies in schizophrenia, which investigated a total of 407 patients, Ellison-Wright and Bullmore (2009) found 2 significantly reduced WM clusters in the left hemisphere: The cerebello-thalamo-cortical circuit and a temporal network interconnecting the frontal lobe, insula, hippocampus (HIP)–amygdala (AMYG), and temporal and occipital lobes, indicating macrocircuit WM changes in schizophrenia. It has also been revealed that reductions in WM tissue proportion extending along much of the large anterior–posterior frontal tracts in the right hemisphere (Shapleske et al. 2002). Despite these observations, to date, magnetic resonance imaging (MRI) studies of aberrant WM lateralization in schizophrenia have not been as informative and conclusive as studies of GM abnormalities (Kubicki et al. 2007; Kubicki and Shenton 2014). Moreover, most previous studies have focused on specific interregional asymmetries in a pairwise manner, specifically, identifying which connections were more coherent or stronger in one hemisphere relative to the other, whereas the effects of these focal laterality changes on wider neural network asymmetry have yet to be determined.

A recent conceptualization suggests that the human brain forms a large-scale network of interconnected regions within the human connectome that provides the anatomical substrate for neural communication, functional processing, and information integration in the brain (Sporns 2011). Graph theoretical analysis has enabled quantitative mapping of this anatomical network at different scales of investigation, and has recently been applied to the study of brain networks in health and disease (Bassett and Bullmore 2009; Bullmore and Sporns 2009; He and Evans 2010; Fornito et al. 2012; Griffa et al. 2013; Stam 2014; van den Heuvel and Fornito 2014). Studies of structural brain networks in schizophrenia at different stages of the disorder have found the presence of the optimal small-world properties (high local clustering and short paths between brain regions), but also the presence of reduced overall structural connectivity (Zalesky et al. 2011; Wang et al. 2012; Zhang et al. 2015), increase of minimum path length (Zhang et al. 2012; Ottet et al. 2013), loss of hubs (brain regions with high interconnectivity) mainly in frontal regions (Bassett et al. 2008; van den Heuvel et al. 2010), and an abnormal rich club (highly interconnected hubs) organization (van den Heuvel et al. 2013). Moreover, the correlation between clinical symptoms and abnormal network organization has also been demonstrated (van den Heuvel and Fornito 2014). Increasingly, schizophrenia is becoming viewed as a disorder of brain dysconnectivity or a disorder of brain network organization because the heterogeneous clinical presentation of schizophrenia (i.e., disorganized, positive, and negative symptoms) may arise from variability in abnormalities of interregional interactions rather than from abnormality in a specific region (Bullmore et al. 1997; Friston 1998; McGlashan and Hoffman 2000; Stephan et al. 2009; Pettersson-Yeo et al. 2011; Fornito et al. 2012; Uhlhaas 2013; van den Heuvel and Fornito 2014; Wheeler and Voineskos 2014). It is noteworthy that the reported aberrations in structural networks of schizophrenia are revealed exclusively at a "whole-brain" level. A few studies have examined network topological organization at the hemispheric level in either healthy young adults or neonates only (Iturria-Medina et al. 2011; Tian et al. 2011; Ratnarajah et al. 2013). For instance, using DTI tractography (a technique to reconstruct WM fiber pathways) and a graph theory framework, Iturria-Medina et al. (2011) recently investigated differences in network architecture between the 2 hemispheres (containing the same number of homologue cortical and subcortical brain regions) in healthy right-handed adults. They found that the right hemisphere is, at the "whole-hemisphere" level, more efficient and interconnected, whereas the left hemisphere presents, at the sub-hemisphere regional level, more central/indispensable regions for the whole-brain structural network, which presumably relates to the leading role of left hemisphere in specific

Downloaded from https://academic.oup.com/cercor/article/27/1/602/3056183 by guest on 11 October 2020

highly demanding cognitive processes, such as language and motor actions. More recently, Ratnarajah et al. (2013) utilized similar analysis framework to investigate structural connectivity asymmetry of the neonatal brain and found optimal small-world characteristics which did not differ between both hemispheres. Moreover, a leftward asymmetric efficiency at both global and local levels was found in the neonatal brain, which may reflect the early development of lateralized functional needs (e.g., perceptual, language, and motor functions) at birth.

To date, no study has reported hemisphere-related differences in the topological organization of brain structural networks in patients with schizophrenia. Given that converging evidence shows aberrant hemispheric asymmetries of various brain regions as well as WM tracts (Ribolsi et al. 2009; Oertel-Knochel and Linden 2011; Miyata et al. 2012; Ribolsi et al. 2014) and impaired structural connectivity in schizophrenia (Ellison-Wright and Bullmore 2009; Stephan et al. 2009; Pettersson-Yeo et al. 2011; Zalesky et al. 2011; Kubicki and Shenton 2014), determining the status of broader structural network asymmetries between the hemispheres may lead to a better understanding of the underlying nature of altered laterality and potentially help to elucidate the etiology of the disorder. In this exploratory study, we employed the DTI deterministic tractography method and a standard graph theory framework to investigate, for the first time, the hemispheric asymmetries of structural brain networks in schizophrenia. In particular, we focused on graph measures of small-world properties (e.g., clustering coefficient, characteristic path length, and small-worldness), global and local network efficiencies, and relative nodal centrality to examine (1) the nature of hemispheric asymmetry of brain connectome in schizophrenia and (2) whether there was association between the abnormal hemispheric asymmetries of network organization and clinical variables.

Materials and Methods

Subjects

In this study, 116 patients with schizophrenia (male/female = 80/36, age = 33.0 ± 9.2 years) and 66 age- and gender-matched normal subjects (male/female = 40/26, age = 31.5 ± 9.9 years) were recruited at the Institute of Mental Health (IMH), Singapore and the local community by advertisements, respectively. All subjects were right-handed according to the Modified Edinburgh Questionnaire (Schachter et al. 1987). The diagnosis evaluation of schizophrenia was performed by a board-certificated psychiatrist (K.S.) using the information obtained from the clinical history, mental status examination, existing medical records, interviews with significant others, as well as the administration of the Structural Clinical Interview for DSM-IV (diagnostic and statistical manual of mental disorders, 4th edition, revised) disorders-Patients Version (SCID-P). Patients and comparison subjects were excluded if they had any of the following characteristics: (1) A history of any significant neurological illness such as brain trauma, epilepsy, or cerebral vascular accident and (2) met DSM-IV criteria for alcohol or other substance abuse. The healthy controls were additionally screened for family history of mental illness: Participants with a first-degree relative suffering from a mental illness would be excluded in this study.

This study was approved by the Institutional Review Board of the IMH, Singapore as well as the National Neuroscience Institute (NNI), Singapore, and informed consent was obtained from each participant. At the time of scanning, all patients were regularly receiving antipsychotic medication and had no changes to their medications for the last 4 weeks. In Table 1, we present the detailed demographics and clinical characteristics of the participants. The antipsychotic medication dosage was converted to daily chlorpromazine milligram equivalents. The positive and negative symptoms scale (PANSS) was used to assess the psychopathology and symptom severity (Kay et al. 1987).

Data Acquisition

Structural MRI scans were performed on a 3-T whole body scanner (Philips Achieva, Philip Medical System, Eindhoven, The Netherlands) with an eight-element SENSE receiver head coil at National Neuroscience Institute, Singapore. Prior to the scanning, subjects were instructed to keep still and remain as motionless as possible. Prescan training and practice were performed to achieve increased patient cooperation. During the data acquisition, subjects lay supine with the head snugly fixed by foam pads provided by the scanner manufacturer to further minimize head motion. One high-resolution T_1-weighted MRI volume images and 3 volumes of diffusion-encoded images were obtained in a single session without altering a position. Specifically, a T_1-weighted magnetization-prepared rapid gradient recalled

Table 1 Demographic and clinical characteristics of the samples[a]

Characteristic	Group (patients/controls = 116/66)		Statistical test	
	Patients with schizophrenia	Normal controls		
Age (years)	18–58 (33.0 ± 9.2)	22–58 (31.5 ± 9.9)	$t_{180} = 1.04$	$P = 0.30$[b]
Male/female	80/36	40/26	$\chi^2_1 = 1.40$	$P = 0.24$[c]
Education (years)	5–18 (11.7 ± 2.5)	9–20 (14.0 ± 1.9)	$t_{180} = -6.49$	$P < 0.001$[b]
Age of onset (years)	15–58 (26.3 ± 7.9)	—	—	—
Duration of illness (years)	1–36 (6.7 ± 7.5)	—	—	—
Medication dose (mg/day)[d]	25–1000 (210.7 ± 203.4)	—	—	—
PANSS positive symptoms[e]	7–22 (10.6 ± 3.6)	—	—	—
PANSS negative symptoms	7–18 (8.9 ± 2.6)	—	—	—
PANSS general symptoms	16–34 (20.2 ± 3.4)	—	—	—

[a]Unless otherwise indicated, data are expressed as a range of minimum–maximum (mean ± SD).
[b]The P-value was obtained using a two-sample two-tailed *t*-test.
[c]The P-value was obtained using a two-tail Pearson χ^2 test.
[d]The antipsychotic medication dosage was converted to daily chlorpromazine milligram equivalents.
[e]The PANSS (Kay et al. 1987) was used to assess the psychopathology and symptom severity.

Downloaded from https://academic.oup.com/cercor/article/27/1/602/3056183 by guest on 11 October 2020

sequence (repetition time [TR] = 7.2 s; echo time [TE] = 3.3 ms; flip angle = 8°) was utilized to obtain high-resolution T_1-weighted MRI volume images (each volume contains 180 gapless axial slices of 0.9 mm thickness, field of view [FOV] = 230 × 230 mm^2; acquisition matrix = 256 × 256; in-plane resolution = 0.9 × 0.9 mm^2) in the direction of the anterior–posterior commissures (AC–PC). A single-shot echo-planar sequence (TR = 3275 ms; TE = 56 ms; flip angle = 90°; *b*-factor = 800 s/mm^2; 1 baseline image with $b0 = 0$ s/mm^2) from 15 separate nonparallel directions was utilized to obtain diffusion-encoded images (each volume containing 42 slices, 3.0 mm with no gap; FOV = 230 × 230 mm^2; acquisition matrix = 112 × 109, reconstructed to 256 × 256). For each participant, the diffusion sequences were scanned 3 times to improve the signal-to-noise ratio (SNR).

Data Preprocessing and Network Construction

Prior to the data preprocessing, the recorded images were visually inspected by experienced radiologists and data with significant head movements were excluded from the current study. Data preprocessing and brain network construction were conducted using FMRIB Software Library (FSL, v5.0; Smith et al. 2004), diffusion toolkit (Wang et al. 2007), and PANDA (a pipeline tool for diffusion MRI analysis; Cui et al. 2013). Specifically, data preprocessing approaches included correction for simple head motion and eddy current distortions using affine transformation to the *b*0 image (Jenkinson et al. 2002). After correction, the 6 independent components of the diffusion tensor were estimated from which fractional anisotropy (FA, a DTI measurement) was calculated. A deterministic streamline tracking algorithm was subsequently performed to obtain the whole-brain fiber tractography (Mori et al. 1999). The tracking procedure started from the deep WM regions and terminated at a voxel with a turning angle greater than 45° or reached a voxel with an FA of <0.15.

The method used here to estimate the brain anatomical networks was similar to the procedure adopted by Gong, He, et al. (2009). Nodes are the fundamental building blocks constituting brain network construction. In this study, we matched 90 cortical and subcortical regions (45 in each hemisphere) to the respective nodes according to the automated anatomical labeling (AAL) parcellation scheme (Tzourio-Mazoyer et al. 2002). The names and corresponding abbreviations of the cortical regions were listed in Supplementary Table 1. A linear transformation was applied locally within each subject's DTI image correlated with T_1-weighted image to coregister them to the *b*0 image with DTI space followed by applying a nonlinear transformation to map to the ICBM152 T1 template [Montreal Neurological Institute (MNI)]. Then, the subject-specific AAL mask was weaved from the MNI space to the DTI native space with the corresponding inverse transformation, such that separate labeling values were maintained via nearest-neighbor interpolation (Gong, He, et al. 2009; Cui et al. 2013). From the reconstructed fiber tracts, edge weight was computed as the number of fiber tracts connecting 2 regions (Shu et al. 2011; Bai et al. 2012). Prior to the fiber bundles counting, WM voxels in the native AAL mask were removed if no cortical voxels existed within their 2-mm cubic neighborhood (Gong, He, et al. 2009). To reduce the influence from pseudoconnections due to possible noise effects on the whole-brain tractography, a predefined threshold was chosen: If the fiber number between the 2 regions was larger than 3; these 2 regions were considered connected (Shu et al. 2011). As such, each individual weighted brain network reflected a symmetric matrix (90 × 90) representation of an individual brain network. Each hemispheric brain network (45 × 45) was then obtained through eliminating the interhemispheric connections. Further network analysis was based on the 2 sets of 45 × 45 weighted networks for each subject. A schematic flowchart of the data analysis was shown in Supplementary Figure 1.

Network Analysis

The network architecture was then investigated at both global and regional levels for the constructed WM networks. Small-world properties were originally proposed by Watts and Strogatz (1998) as having higher local clustering and equivalent characteristic path length compared with the random networks. In this work, we calculate small-world parameters of the weighted brain networks (including weighted clustering coefficient, C_w; weighted characteristic path length, L_w; small-worldness, σ). To further provide a clear and direct physical meaning to the concept of small-world properties in terms of information flow (Latora and Marchiori 2001; Achard and Bullmore 2007), global efficiency, E_{global}; and local efficiency, E_{local}, were also estimated. Regional properties were described in terms of nodal efficiency, $E_{nodal}(i)$ (Achard and Bullmore 2007). Here, we provided definitions and brief interpretations of the parameters (Table 2). Greater details of the descriptions of the graph theoretical parameters could be found in Supplementary Material and reviews of this topic (Boccaletti et al. 2006; Bullmore and Sporns 2009; Rubinov and Sporns 2010). The graph theoretical analysis was conducted using the Brain Connectivity Toolbox (Rubinov and Sporns 2010).

Asymmetry Score

Brain network asymmetry of the aforementioned network metrics was evaluated by the asymmetry score (Iturria-Medina et al. 2011; Ratnarajah et al. 2013): $AS(X) = 100 \times [X(R) - X(L)]/[X(R) + X(L)]$, where $X(R)$ and $X(L)$ are the network parameters of the right and left hemispheres, respectively. Through incorporating the relative network metrics over both hemispheres in one value, the $AS(X)$ index allows us to look at differences between the right and left hemispheres. The $AS(X)$, ranging between +100 and −100, is positive when metric X showed prominent rightward asymmetry and negative when the opposite is the case. (L_w measures the overall routing efficiency of the network and is inversely related to E_{global}. For a network, the higher of L_w, the lower efficient of the global integration. Hence, positive $AS(L_w)$ indicates a leftward advantage of global integration and negative $AS(L_w)$ represents rightward asymmetry of global integration.)

Statistical Analysis

Between-Group Differences

Data were first checked for normality and transformed when necessary to meet the assumption of normality. To test the group differences in age and years of education, data was analyzed with separate two-tailed *t*-tests. The gender data were analyzed using a χ^2 test. To assess hemispheric effects on the network properties between 2 groups, a general linear model (GLM) comprising hemisphere as a within-subject factor, group as a between-subject factor, and group-by-hemisphere as interaction, was performed on the obtained network metrics. Given that hemispheric asymmetry is associated with normal aging (Cabeza 2002) and sexual dimorphism (Good et al. 2001); age, gender, and age-by-gender interaction were set as covariates in this work. If any effect was significant, further post hoc tests were performed (paired *t*-test for hemisphere effect and two-sample two-tailed

Downloaded from https://academic.oup.com/cercor/article/27/1/602/3056183 by guest on 11 October 2020

Table 2 Formulations and description of topological measurements applied in the current work

Network properties	Definitions	Measurement and meaning
Clustering coefficient (C_w)	$C_w = \frac{1}{N}\sum_{i\in N}\frac{\sum_{j,k}(\bar{w}_{ij}\bar{w}_{jk}\bar{w}_{ki})^{1/3}}{(k_i(k_i-1))}$	C_w measures the extent of a local density or cliquishness of a network G with N nodes ($N = 45$ in this study). Here, k_i is the number of edges connecting to node i, $\bar{w}_{ij}$ is the edge weight between region i and j, which is scaled by the mean of all weights to control each participant's cost at the same level.
Characteristic path length (L_w)	$L_w = \frac{1}{N(N-1)}\sum_{i\in N}\sum_{i\neq j\in N}\min\{L_{ij}\}$	L_w measures the overall routing efficiency of the network. $\min\{L_{ij}\}$ is the shortest path length between node i and j.
Small-worldness (σ)	$\sigma = \frac{\gamma}{\lambda} = \frac{C_w/C_w^{rand}}{L_w/L_w^{rand}}$	σ measures the small-world property. $C_w{}^{rand}$ and $L_w{}^{rand}$ represent the mean indices derived from 100 matched random networks. These random networks were derived from the original brain network by randomly rewiring the edges between nodes while preserving the degree distribution and connectedness.
Global efficiency (E_{global})	$E_{global} = \frac{1}{N(N-1)}\sum_{i\neq j\in G}\frac{1}{\min\{L_{ij}\}}$	E_{global} is a measure of the global efficiency of parallel information transfer in the network. It is inversely related to L_w.
Local efficiency (E_{local})	$E_{local} = \frac{1}{N}\sum_{i\in G}E_{global}(i)$	E_{local} measures the mean local efficiency of the network.
Nodal efficiency (E_{nodal})	$E_{nodal}(i) = \frac{1}{N}\sum_{i\neq j\in G}\frac{1}{\min\{L_{ij}\}}$	$E_{nodal}(i)$ is the inverse of the harmonic mean of the shortest path length between node i and all other nodes. It measures the ability of information transmission of node i in the network: A node with high E_{nodal} indicates great interconnectivity with other regions in the network.
Normalized E_{nodal} ($\overline{E_{nodal}}$)	$\overline{E_{nodal}}(i) = \frac{N\times\sum_{s=1}^{M}E_{nodal}(i,s)}{\sum_{i=1}^{N}\sum_{s=1}^{M}E_{nodal}(i,s)}$	$\overline{E_{nodal}}$ is the normalized nodal efficiency and M is the number of subjects in each group ($M_{NC} = 66$ and $M_{SCZ} = 116$). Region i was considered as the hub if $\overline{E_{nodal}}(i)$ was at least 1 SD higher than the average of the metrics over the network ($\overline{E_{nodal}}(i) >$ mean + SD).

t-test for group effect). For the asymmetry score, a two-tailed one-sample t-test was initially utilized to determine whether the AS of the network metrics within each group was significantly different from zero. A univariate analysis of covariance (ANCOVA) was then performed on the AS to assess the group effect. Age, gender, and age-by-gender interaction were also controlled. A value of $P < 0.05$ was considered significant. Corrections for multiple comparisons of nodal characteristics were performed via Bonferroni correction ($P < 0.05/45$). All statistical analyses were performed using the SPSS 17 software.

Relationship Between Network Metrics and Clinical Variables

Relationships between the hemispheric asymmetry scores and clinical variables were also explored in the patients with schizophrenia. Specifically, multiple linear regressions were employed and implemented in the statistical package, R (http://www.r-project.org/) in the current study, with the covariates of age, gender, age-by-gender, and medication. To limit the number of association calculations for regional properties, only network metrics that displayed significant hemispheric asymmetry in the test of asymmetry scores were chosen as independent variables. Because these analyses were exploratory in nature, correction for multiple comparisons was not applied, and an uncorrected P-value of 0.05 was considered for establishment of a significant relationship.

Results

Global Properties of Hemispheric Networks

Hemispheric and Group Effects

In the current study, the structural organization of hemispheric networks was investigated rather than the whole brain. We found that the hemispheric brain structural connectome of both groups exhibited prominent features of small-world topology, as expressed by a much higher local clustering than random networks and a comparable short characteristic path length of the random networks (see Supplementary Fig. 2). Nonetheless, quantitative statistical analyses revealed significant topological changes in the global network metrics between both groups and hemispheres (Table 3). Significant group effects were observed in the weighted characteristics path length, L_w, (NC < SCZ, $F_{1,\ 177} = 9.556$, $P = 0.002$) and global efficiency, E_{global}, (NC > SCZ, $F_{1,\ 177} = 9.387$, $P = 0.003$), indicating a hemispheric-independent global integration deficit in patients with schizophrenia. Furthermore, hemispheric effect was highly significant for L_w, (right < left, $F_{1,\ 180} = 10.045$, $P = 0.002$), small-worldness, σ, (right < left, $F_{1,\ 180} = 28.879$, $P < 0.001$), E_{global}, (right > left, $F_{1,\ 180} = 13.186$, $P < 0.001$), and local efficiency, E_{local}, (right > left, $F_{1,\ 180} = 23.108$, $P < 0.001$). Specifically, the right hemisphere exhibited better global and local information transfer efficiency, whereas the left hemisphere showed more optimal small-world architecture. More importantly, a significant group-by-hemisphere interaction was revealed on L_w ($F_{1,\ 180} = 5.443$, $P = 0.021$) and E_{global} ($F_{1,\ 180} = 5.108$, $P = 0.025$). Post hoc analysis indicates that this interaction resulted from a significant rightward predilection of global integration in healthy participants ($P < 0.001$) and a symmetric pattern in patients (Fig. 1).

The Asymmetry Score

Statistical analysis results of the asymmetry scores of the global network metrics were summarized in Table 4. For both groups, the right hemisphere tended to be more efficient for local information transfer [positive $AS(E_{local})$, $P = 0.001$], whereas a left hemispheric advantage in the small-world properties [negative

Downloaded from https://academic.oup.com/cercor/article/27/1/602/3056183 by guest on 11 October 2020

AS(σ), $P < 0.001$] was also observed. Moreover, a right hemispheric predilection of global efficiency (L_w, $t_{65} = -3.494$, $P < 0.001$; E_{global}, $t_{65} = 3.489$, $P < 0.001$) was only observed in normal controls. Asymmetry scores of global network metrics for each individual were shown in Supplementary Figure 3. When comparing the asymmetry scores of the global network metrics between 2 groups, L_w ($F_{1,\ 177} = 5.664$, $P = 0.018$) and E_{global} ($F_{1,\ 177} = 4.975$, $P = 0.027$), exhibited significant differences in asymmetry scores, which were consistent with the above results of significant group-by-hemisphere interaction revealed by a GLM model. This finding further highlighted a significantly reduced hemispheric asymmetry in patients that the patterns of right-more-than-left efficient global integration seen in healthy controls were not observed in patients with schizophrenia.

Regional Nodal Properties of the Hemispheric Networks

Hemispheric and Group Effects

Using GLM statistical analyses, we further localized the regions showing statistical hemispheric differences between patients and controls (Fig. 2 and see Supplementary Table 3). Significant hemispheric effects ($P < 0.05$, Bonferroni-corrected) were observed in 26 regions across the cerebral cortex (Fig. 2A). Among these brain regions, 10 regions (including the anterior cingulate gyrus [ACG], the AMYG, the inferior frontal gyrus, triangular part [IFGtriang], the inferior frontal gyrus, opercular part [IFGoperc], the inferior parietal lobe [IPL], the middle occipital gyrus [MOG], the olfactory [OLF], the orbitofrontal gyrus, medial part [ORBmed], the postcentral gyrus [PoCG], and the superior frontal gyrus medial part [SFGmed]) mainly resided in the inferior frontal and parietal areas showed leftward predilection in regional efficiency, whereas 16 regions (including the angular gyrus [ANG], the caudate nucleus [CAU], the cuneus [CUN], the fusiform gyrus [FFG], the HIP, the inferior temporal gyrus [ITG], the middle temporal gyrus [MTG], the orbitofrontal gyrus, inferior part [ORBinf], the orbitofrontal gyrus, middle part [ORBmid], the pallidium [PAL], the precuneus [PCUN], the parahippocampal gyrus [PHG], the putamen [PUT], the superior temporal gyrus [STG], the temporal pole, middle part [TPOmid], and the temporal pole, superior part [TPOsup]), predominantly located in the temporal and orbitofrontal regions, exhibited a rightward advantage in regional efficiency (see Supplementary Table 3). Furthermore, a significant group effect (NC > SCZ, $P < 0.05$, Bonferroni-corrected) on the nodal efficiency was revealed in the FFG, the IPL, the PHG, the STG, and the ITG (Fig. 2B). Moreover, a significant group-by-hemisphere interaction was revealed in the IFGoperc ($F_{1,\ 180} = 11.452$, $P = 0.001$), the SFGmed ($F_{1,\ 180} = 11.675$, $P = 0.001$), and the HIP ($F_{1,\ 180} = 10.735$, $P = 0.001$; Fig. 2C). Trend-wise group-by-hemisphere interaction was also revealed in the IPL ($F_{1,\ 180} = 5.007$, $P = 0.026$) and the STG ($F_{1,\ 180} = 5.910$, $P = 0.016$). Post hoc analysis indicates that most of the interaction effects (4 out of 5) resulted from a significantly reduced hemispheric asymmetry of regional efficiency in schizophrenia (see Supplementary Fig. 5).

Table 3 Group and hemispheric effects on the global network metrics

Metrics	General linear mixed model		
	Group effect $F_{1,177}$ (*P*-value)	Hemisphere effect $F_{1,180}$ (*P*-value)	Interaction $F_{1,180}$ (*P*-value)
C_w	0.067 (0.796)	1.676 (0.197)	1.291 (0.257)
L_w	**9.566 (0.002)** $^{\downarrow}$	**10.045 (0.002)** $^{\blacktriangledown}$	**5.443 (0.021)**
σ	0.494 (0.483)	**28.879 (<0.001)** $^{\blacktriangledown}$	0.757 (0.385)
E_{global}	**9.387 (0.003)** $^{\uparrow}$	**13.186 (<0.001)** $^{\blacktriangle}$	**5.108 (0.025)**
E_{local}	2.025 (0.156)	**23.108 (<0.001)** $^{\blacktriangle}$	1.018 (0.314)

Note: The statistical results were computed with a GLM comprising hemisphere as a within-subject factor, group as a between-subject factor, and group-by-hemisphere as interaction. The effects of age, gender, and age-by-gender interaction were controlled for all of these analyses. Significant effects ($P < 0.05$) were indicated by the bold text.

SCZ, schizophrenia; NC, normal control; $^{\downarrow}$, NC < SCZ; $^{\uparrow}$, NC > SCZ; $^{\blacktriangledown}$, right < left; $^{\blacktriangle}$, right > left.

The Asymmetry Score

In agreement with prior linear mixed model results, significant hemispheric asymmetry was also observed in the nodal efficiency for both groups. Specifically, 15 nodes in the hemispheric networks of normal controls (Fig. 3A) and 19 nodes in the networks of patients with schizophrenia (Fig. 3B) were significantly ($P < 0.05$, Bonferroni-corrected) asymmetric. The distribution of these asymmetric regions and the direction of the asymmetries were in agreement with previous GLM hemispheric results. When comparing the asymmetry scores of the regional properties between patients and healthy participants, significant between-group differences ($P < 0.05$, Bonferroni-corrected) were revealed in the IFGoperc, attributing to the reduced left hemispheric predilection of regional efficiency in patients with schizophrenia. In addition, several regions exhibited trends of differences, including the SFGmed ($F_{1,\ 177} = 9.748$, $P = 0.002$), the HIP ($F_{1,\ 177} = 7.901$, $P = 0.005$), and the STG ($F_{1,\ 177} = 4.989$, $P = 0.027$). These results were compatible with the significant group-by-hemispheric interaction on the regional nodal efficiency revealed in the linear mixed model.

Relationship Between Hemispheric Asymmetry and Clinical Features

Within the schizophrenia group, the asymmetry scores of the characteristic path length and global efficiency correlated

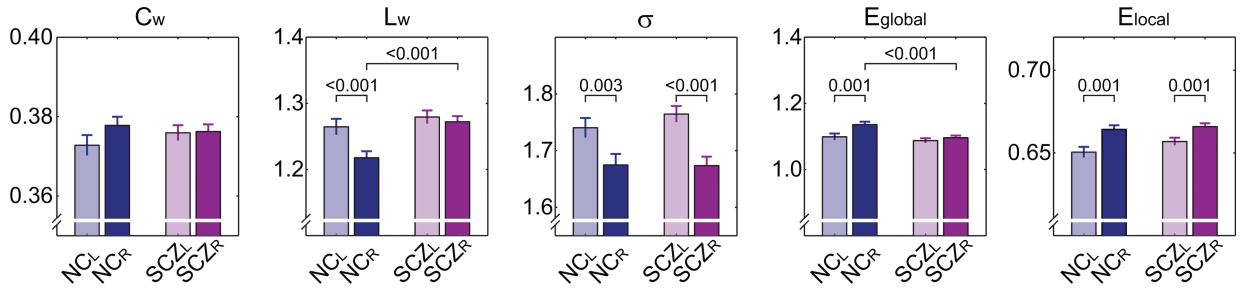

Figure 1. Post hoc statistical analysis of global network metrics. Bars represent mean ± SD. Each horizontal line and associated number represent the *P*-value of a *t*-test (paired *t*-test for hemispheric effect at each group and two-sample *t*-test for group effect).

Downloaded from https://academic.oup.com/cercor/article/27/1/602/3056183 by guest on 11 October 2020

significantly with the disease duration ($AS(L_w)$, $r = 0.207$, $P = 0.029$; $AS(E_{global})$, $r = -0.224$, $P = 0.018$). Of note, the global efficiency and characteristic path length are inversely related, hence leading to converse correlations for both. In addition, the asymmetry scores of small-worldness, $AS(\sigma)$, exhibited a significant positive correlation with the PANSS positive symptoms ($r = 0.226$, $P = 0.017$). For the regional asymmetry scores, 5 nodes (including the OLF, the ORBmed, the ACG, the TPOsup, and the ITG) exhibited significant ($P < 0.05$) correlations with the clinical measurements (Table 5). Specifically, a significant negative correlation was observed between the asymmetry scores of nodal efficiency in the OLF, the ORBmed, and the TPOsup and the disease duration. For the PANSS positive symptoms, significant correlations were found in the ORBmed [AS(ORBmed), $r = 0.200$, $P = 0.035$] and the ITG [AS(ITG), $r = -0.213$, $P = 0.024$]. For the PANSS negative symptoms, only the ACG exhibited significant positive correlation [AS(ACG), $r = 0.243$, $P = 0.010$].

Table 4 Group effect on the asymmetry scores of the global network metrics

Metrics	Patients with SCZ t_{115} (*P*-value)	NC subjects t_{65} (*P*-value)	SCZ versus NC $F_{1,177}$ (*P*-value)
$AS(C_w)$	0.168 (0.867)	1.467 (0.147)	1.388 (0.240)
$AS(L_w)$	−0.579 (0.564)	**−3.494 (<0.001)**	**5.664 (0.018)**
$AS(\sigma)$	**−5.072 (<0.001)**	**−3.296 (0.002)**	0.856 (0.356)
$AS(E_{global})$	1.267 (0.208)	**3.489 (<0.001)**	**4.975 (0.027)**
$AS(E_{local})$	**3.392 (0.001)**	**3.383 (0.001)**	1.263 (0.263)

Note: The statistical results within each group were obtained via a one-sample two-tailed *t*-test. A univariate ANCOVA was performed on the *AS*s to further assess the between-group differences, and the effects of age, gender, and age-by-gender interaction were controlled for all of these analyses. Positive *t*-values within each group indicate rightward asymmetries and vice versa. Bold indicates variables that are statistically significant ($P < 0.05$).
SCZ, schizophrenia; NC, normal control.

Discussion

To the best of our knowledge, this is the first study examining hemispheric asymmetry in brain WM topological networks in patients with schizophrenia using DTI and graph theory. The significant findings are as follows: first, although small-world characteristics were preserved in the hemispheric network, a significant overall deficit of global integration was found in patients with schizophrenia; second, a significant group-by-hemisphere interaction was revealed in the characteristic path length and global efficiency, attributing to a significantly reduced hemispheric asymmetry of global integration in patients compared with healthy controls; third, several specific brain regions (including the IFGoperc, the HIP, the IPL, and the STG) exhibited a reduced asymmetric nodal efficiency in patients with schizophrenia; and fourth, the aberration of hemispheric network topological properties was correlated with the clinical features of schizophrenia.

The identification of small-world topology has made a great impact on our understanding of the topological organization of

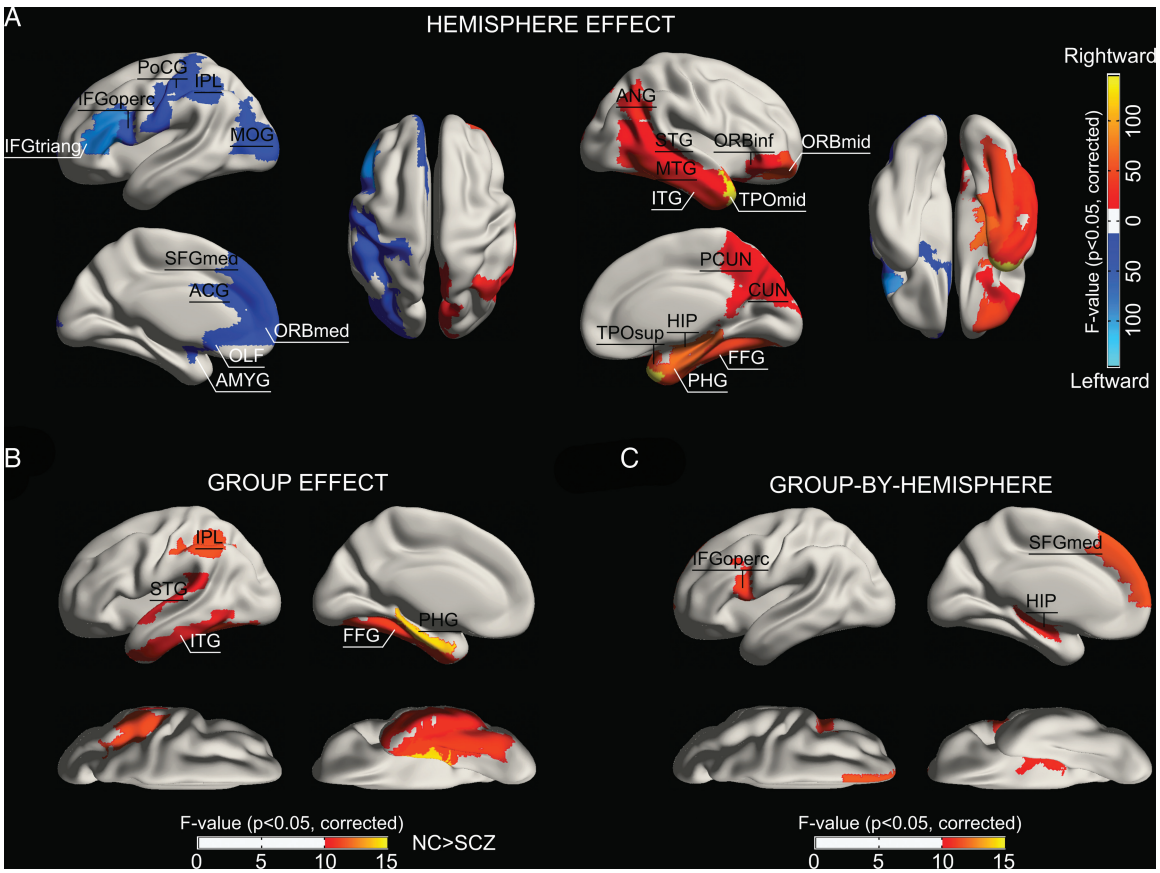

Figure 2. The surface spatial distribution of cortical regions showing significant (*A*) hemispheric effect, (*B*) group effect, and (*C*) group-by-hemispheric interaction on the nodal characteristics. The color bar represents *F*-values. The threshold value for establishing significance was set at $P < 0.05$ (Bonferroni-corrected). Significant regions were overlaid on inflated surface maps with BrainNet Viewer software (Xia et al. 2013). For the abbreviations of the cortical regions, see Supplementary Table 1.

Downloaded from https://academic.oup.com/cercor/article/27/1/602/3056183 by guest on 11 October 2020

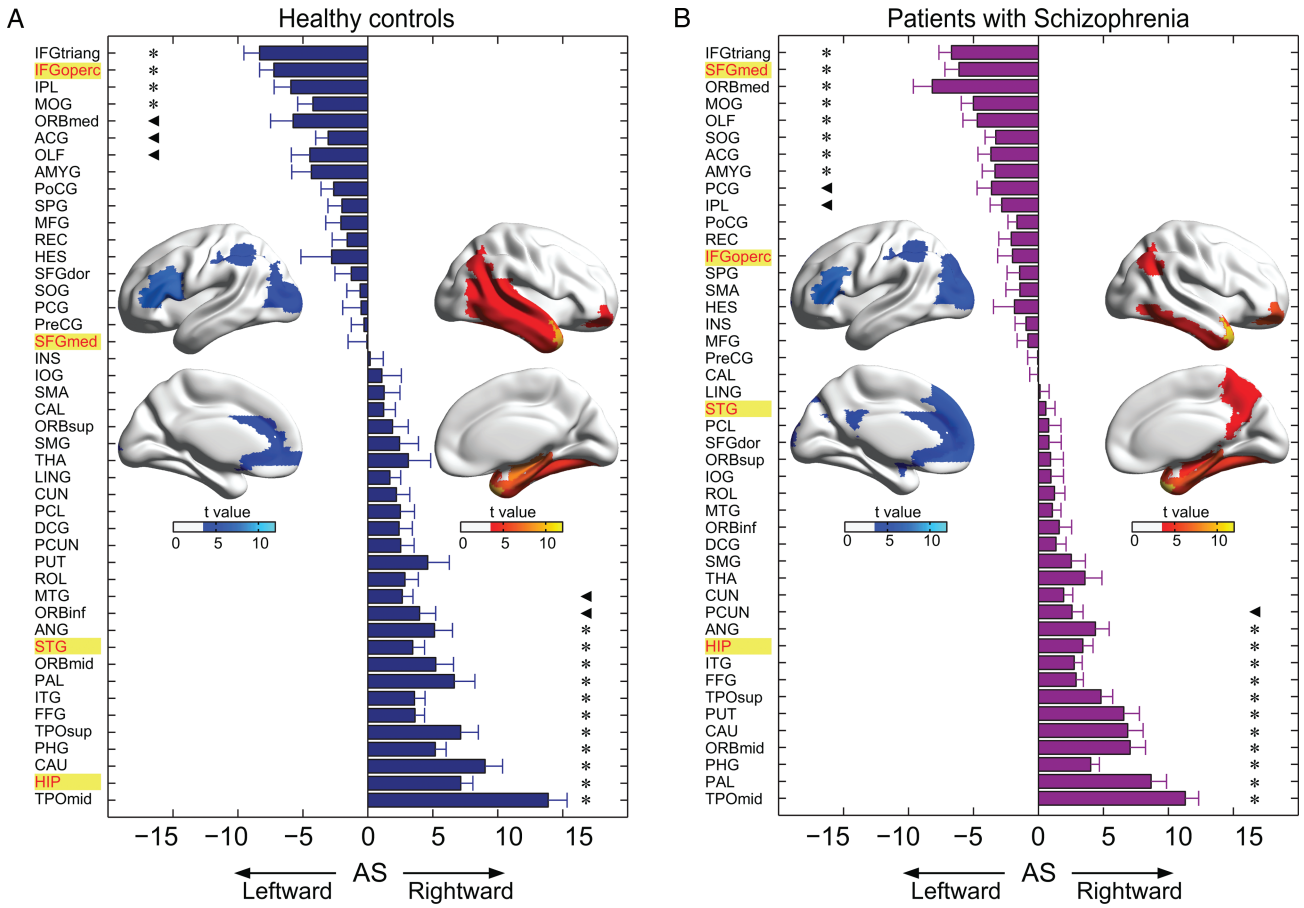

Figure 3. The asymmetry scores of nodal efficiency for the 45 ROIs. Each bar represents the mean asymmetry scores (*AS*). Error bars denote standard error. Regions with significant (*P < 0.05, Bonferroni-corrected; ◄P < 0.005, uncorrected) asymmetry scores in (*A*) normal control participants and (*B*) patients with schizophrenia are indicated with asterisk. The regions were sorted by the ascending of statistical *t*-values in each group. The spatial distributions of cortical regions showing significant AS in both groups were also presented with BrainNet Viewer software (Xia et al. 2013). The color bar shows *t*-values. Brain regions with significant group difference were highlighted (yellow background). For the abbreviations of the cortical regions, see Supplementary Table 1.

brain networks (Bullmore and Sporns 2009; Sporns 2011). In particular, small-world architecture is characterized by high local clustering of connections between neighboring brain regions but with short path length, representing a balance between local specialization/necessities (fault tolerance) and global integration of brain functional activity. Moreover, this neural architecture has the capacity to process information in parallel, which is computationally much more efficient than serial or hierarchical processing. In the "whole-brain" level, convergent evidence has shown the presence of the small-world network properties in healthy subjects and in patients with schizophrenia (Bullmore and Sporns 2009; Fornito et al. 2012; Uhlhaas 2013; van den Heuvel and Fornito 2014). Our observations extend earlier findings by showing that the individual hemispheres also demonstrate optimal small-world characteristics in both healthy participants and patients with schizophrenia, indicating that information processing within each hemisphere could be of similar efficiency to that of the whole brain.

A significant group main effect was observed in the weighted characteristic path length and global efficiency, that is, patients had longer path length and smaller global efficiency independent of hemisphere, demonstrating a disturbance of the normal balance in the efficient small-world model, specifically suggesting reduced communication between segregated parts of the brain. This finding was consistent with prior observations from functional (Liu et al. 2008) and structural network (Wang et al. 2012; Zhang et al. 2012; Ottet et al. 2013) studies, which have shown less efficient information propagation within brain networks in schizophrenia than in comparable healthy age groups. Contemporary theories suggest that the complex clinical presentations of schizophrenia are related to aberrant, or "dys-," connectivity between distinct brain regions rather than abnormalities within the separate regions themselves, therefore emphasizing the role of the brain's integrative process—the substrate of which is connectivity—in the pathophysiology of schizophrenia (Bullmore et al. 1997; Friston 1998; Stephan et al. 2006). Such a concept can be alternatively described as an aberration in the efficiency of information exchange between separate neural networks in the human brain. Along this line, our findings of "hemispheric-independent" significantly longer path length and smaller global efficiency provide further evidence for the notion of schizophrenia as a disconnection syndrome (Bullmore et al. 1997; Friston 1998; McGlashan and Hoffman 2000; Pettersson-Yeo et al. 2011; Fornito et al. 2012; Uhlhaas 2013; van den Heuvel and Fornito 2014).

In addition, we found that healthy controls exhibited significant right-greater-than-left asymmetry of shorter weighted characteristic path length and better global efficiency, indicating a more optimal global integration in the right hemisphere. In accordance with our observation, Iturria-Medina et al. (2011) found

Downloaded from https://academic.oup.com/cercor/article/27/1/602/3056183 by guest on 11 October 2020

Table 5 Partial correlation coefficients between the global and nodal asymmetry scores and clinical characteristics of patients with schizophrenia

Metrics	Partial correlation coefficients (*P*-value)			
	PANSS positive	PANSS negative	PANSS general	Duration
AS(L_w)	0.017 (0.863)	−0.004 (0.965)	0.056 (0.557)	**0.207 (0.029)**
AS(σ)	**0.226 (0.017)**	−0.184 (0.053)	0.083 (0.384)	−0.112 (0.239)
AS(E_{global})	−0.048 (0.614)	0.126 (0.185)	−0.112 (0.243)	**−0.224 (0.018)**
AS(OLF)	0.050 (0.603)	0.148 (0.121)	0.107 (0.262)	**−0.234 (0.013)**
AS(ORBmed)	**0.200 (0.035)**	0.113 (0.237)	0.034 (0.725)	**−0.193 (0.042)**
AS(ACG)	0.075 (0.434)	**0.243 (0.010)**	0.021 (0.829)	−0.162 (0.088)
AS(TPOsup)	−0.036 (0.707)	0.088 (0.354)	0.018 (0.849)	**−0.277 (0.003)**
AS(ITG)	**−0.213 (0.024)**	0.072 (0.449)	−0.180 (0.058)	−0.023 (0.812)

Note: The partial correlation coefficients were estimated via multiple linear regressions with age, gender, and age-by-gender interaction as covariates. Significant correlations ($P < 0.05$) were indicated by the bold text.
PANSS, positive and negative symptom scale. For the abbreviations of the cortical regions, see Supplementary Table 1.

in their hemispheric structural efficiency study of healthy human and nonhuman primates that the right hemisphere is organized more efficiently independent of the choices of tracking algorithms. According to Iturria-Medina, this rightward asymmetry might reflect the specialization of the right hemisphere for broader processes like visuospatial integration and attentional processing interact, whereas specific cognitive processes, such as language and motor functions, are predominantly carried out in the left hemisphere in normally lateralized individuals (Iturria-Medina et al. 2011). Consistent with this notion, Gotts et al. (2013) reported 2 distinct forms of hemispheric functional lateralization in the human brain, with left hemisphere showing a preference to interact more exclusively with itself, particularly for cortical regions involved in language and fine motor coordination; whereas right hemisphere regions interact in a more integrative fashion with both hemispheres. Interestingly and in line with these studies, we also found a leftward predilection in the regional hubs for healthy participants (left/right = 9/7) (see Supplementary Material). Using voxel-based analysis, Barrick et al. (2005) revealed a rightward asymmetry in the WM volume for healthy adults, which was further validated in Herve et al. (2006). Given the role of WM in coordinating communication between different brain regions, this hemispheric asymmetry in WM volume may underlie the rightward global integration in healthy controls. Significantly, such rightward advantage of global integration in healthy individuals was absent in patients with schizophrenia; instead, a symmetric pattern of global integration at "whole-hemisphere" level was observed. In previous neuroimaging (Bilder et al. 1994; DeLisi et al. 1997; Collinson et al. 2003; Park et al. 2004; Takao et al. 2010; Ribolsi et al. 2014) and postmortem studies (Crow et al. 1989; Falkai et al. 1995; Highley et al. 1999), there is a considerable amount of evidence for reduced focal asymmetry in schizophrenia. While exploratory, our finding adds to earlier work and provides connectomic evidence that schizophrenia is associated with abnormal lateralization at the "whole-hemisphere" level, particularly a deficit of global integration in the right hemisphere. Most recently, in one meta-analysis of WM deficits in first-episode schizophrenia investigating 8 studies with a total of 271 patients, Yao et al. (2013) found consistent FA reductions in the WM of the right anterior cingulate region. This region contains the anterior cingulum bundle, which is essential to the limbic circuitry for the integration of external and internal information. While there is no comparable structural data involving hemispheric small-world properties in schizophrenia, our findings are in line with these earlier studies, suggesting that right hemisphere deficits may underlie psychotic psychopathology in schizophrenia (Cutting 1992; Mitchell and Crow 2005).

In contrast to the previous studies, where regional asymmetry was mainly determined from morphologic differences between 2 hemispheres, regional asymmetry was estimated by comparing the regional efficiency of the hemispheric structural network. In line with the well-documented leftward asymmetry in language, motor, and visual functions in right-handed people (Mesulam 1998), we found regions with significant leftward asymmetry included the inferior frontal gyrus, the postcentral gyrus, the inferior parietal gyrus, and the middle occipital gyrus. Moreover, the observed leftward regional asymmetry in the ACG, the OLF, and the SFG was consistent with similar cortical thickness (Luders et al. 2006) and DTI results (Park et al. 2004). The rightward predominance of regional efficiency was found in the regions mainly located in the temporal, parieto-occipital, and orbitofrontal areas, corresponding to the rightward predilection in emotion and in visuospatial and memory functioning (Mesulam 1998). Of note, aberrations of brain regional characteristics are increasingly implicated and thought to underline the neurobiological basis of schizophrenia (Rubinov and Bullmore 2013). In line with findings of previous brain connectome studies (Wang et al. 2010, 2012), we found that schizophrenia was associated with reduced nodal efficiency in regions (including the FFG, the IPL, the PHG, the STG, and the ITG) predominantly in temporal paralimbic and associative cortices. Conceptually, regional efficiency is based on the cortical connectivity patterns and therefore biologically relates to the axonal properties across the cerebral cortex (Gong, Rosa-Neto, et al. 2009). Using DTI, previous studies have reported degenerated anatomical connectivity in temporal-related WM tracts and the WM tracts linking the paralimbic and associative areas (Kanaan et al. 2005; Kubicki et al. 2007; Fitzsimmons et al. 2013), which may represent a part of the reduced regional efficiency observed in this study. More importantly, most of the regions with reduced nodal efficiency were identified as hubs (the left IPL, the bilateral FFG, the STF, and the ITG) in this study (see Supplementary Material) and in previous brain connectome studies (Achard et al. 2006; Wu et al. 2012). Given the central role of hubs in receiving convergent inputs from multiple cortical regions, it seems plausible that profoundly disrupted regional efficiency may indicate more isolated network architecture in schizophrenia, presumably leading to the observed deficits in overall global integration. Additionally, we found a significant group-by-hemisphere interaction in the nodal efficiency of 5 regions (the IFGoperc, the SFGmed, the HIP, the IPL, and the STG), whereby most (4/5) exhibited a pattern of

Downloaded from https://academic.oup.com/cercor/article/27/1/602/3056183 by guest on 11 October 2020

reduced hemispheric asymmetry in patients. Of note, several brain regions, including the IFGoperc, the HIP, the IPL, and the STG, consistently exhibited reduced morphologic and WM asymmetry in schizophrenia (Harrison 2004; Torrey 2007; Ribolsi et al. 2009; Takao et al. 2010). Interestingly, an increased asymmetry was observed in the SFGmed of patients group, attributing to a significant reduced nodal efficiency in the right hemisphere. The SFG is involved in self-awareness and emotion (Fried et al. 1998; Goldberg, et al. 2006). Convergent evidence has shown reduced volume of SFG in patients with schizophrenia (Chan et al. 2011), which is associated with a disturbance of self-awareness and emotion. We speculate the observed asymmetric pattern may indicate a lateralized reduction in the SFG.

Another interesting finding of the current study is that within patients, the aberration of hemispheric network topological properties was associated with duration of illness and clinical symptom ratings on PANSS. Specifically, we found a positive relationship between the duration of disease and the reduced hemispheric lateralization of global integration in schizophrenia; that is, the longer the duration of disease, the longer characteristic path length (smaller global efficiency) in the right hemisphere. This suggests that such attenuated asymmetry in schizophrenia might be a progressive process. However, our findings are unlike one recent study of abnormal asymmetry of voxel-wise WM integrity, which revealed no significant correlation between the abnormal asymmetry and the duration of illness (Miyata et al. 2012). The discrepancies between the 2 studies could stem from the following 2 aspects. First, we investigated the abnormal asymmetry based on the brain connectome properties at the whole-hemisphere level instead of the direct comparisons of regional morphologic changes. Second, a relatively small number of samples ($N = 26$) was enrolled in the early study and many of those included patients were with a chronic illness course. In comparison, a large sample ($N = 116$) of patients ranging from recent first episode to chronic course was included in the current study, which led to our being able to identify association between the reduced hemispheric lateralization of global integration and the duration of disease. In agreement with our observations, a generally attenuated asymmetry was revealed in patients with a chronic course, such that anomalous asymmetry increases with the duration of disease in a recent study investigating functional connectivity asymmetry with high-resolution EEG (Jalili et al. 2010). Further studies may help to reconcile such apparent inconsistencies. In addition, a significant positive association between PANSS positive symptoms and the asymmetry scores of small-worldness was revealed such that the more severe the positive symptoms, the larger small-worldness in the right hemisphere. Positive psychotic symptoms typically encompass delusions and hallucinations (Howes and Murray 2014). Consistent with our observation, previous imaging studies of psychotic symptoms have found a predominantly right hemispheric activation during auditory hallucinations (Sommer et al. 2001) and loss of auditory laterality and left temporal volume in those who have auditory hallucinations compared with those who do not (Collinson et al. 2009). Using the DTI tractography method, Wang et al. (2012) found a significant relationship between the network properties and clinical manifestations of schizophrenia. Likewise, a robust relationship between abnormal brain network topology and schizophrenia clinical symptoms has emerged (van den Heuvel and Fornito 2014). As such, the present findings support a general trend in the literature showing a direct correspondence between clinical symptomatology and the underlying anatomical structures supporting network efficiency and suggest the usefulness of brain network properties as potential biomarkers for diagnosis and evaluation of the severity of the disease as well as understanding the pathophysiologic mechanisms. Of note, given that the statistical significance in this work was assessed without corrections for multiple comparisons, the observed significant relationship between the network metrics and illness dynamics should be interpreted as exploratory in nature. Future longitudinal studies examining the progressive disruptions of brain anatomical networks and its association with clinical variables are of particular interest to reveal the illness progression and clinical changes with treatment.

There are several methodological issues that need to be noted. First, in order to obtain robust and stable findings of abnormal hemispheric asymmetry of brain connectome, a large sample of patients ($N = 116$) was recruited in the current study, which may potentially introduce some confounding factors, such as different medication dosage among patients. Previous neuroimaging studies of schizophrenia have reported pharmacological changes in localized brain regions and connections (Kanaan et al. 2009; Navari and Dazzan 2009; Andreasen et al. 2011). However, in terms of global network properties, evidences pertaining to the association between network measurements and medication dosages are not entirely consistent (Micheloyannis et al. 2006; Liu et al. 2008; Rubinov et al. 2009). In fact, Rubinov et al. (2009) suggested that medication is unlikely to be a confounding factor and may, on the contrary, exert a normalizing influence. These studies therefore lead us to believe that the observed between-group differences may reflect the intrinsic disease process instead of an effect of direct pharmacological treatment. Second, a computationally inexpensive deterministic tractography method was utilized to reconstruct the structural brain networks. This fiber tracking method is generally known to have limited capacity in handling complex fiber architecture (i.e., nonuniform fiber orientation) and may result in potential loss of existing fibers between brain regions or inclusion of some nonexistent fibers (Mori et al. 1999; Li et al. 2009). In terms of network weighting, a measure of fiber number was adopted in the current study. Although widely used (Hagmann et al. 2008; Shu et al. 2011; Zalesky et al. 2011; Bai et al. 2012), the fiber count depends on the features of fiber pathway (i.e., curvature, fiber length, width, and myelination) and is sensitive to the experimental conditions (i.e., local variations in the SNR; Jones 2010; Jones et al. 2013). We assessed the credibility of our tracking results in Supplementary Fig. 6 through showing 8 well-known WM fiber bundles from 2 randomly selected subjects (one patient with schizophrenia and one healthy participant). We found that the reconstructed fiber bundles are faithful to the human WM anatomy from previous studies (Gong, He, et al. 2009; Li et al. 2009). Several recent studies had shown that probabilistic tractography outperformed the deterministic method in overcoming the fiber crossing issue and the robustness to the image noise, in which much higher sampling orientations were typically required (Buchanan et al. 2014). In this study, the DTI images were obtained using 15 nonparallel directions; our credible tracking results suggested that a single tensor model and a deterministic tracking method might be the optimal choice (Wang et al. 2012). Nevertheless, further studies with higher angular data could investigate structural brain networks reconstructed by probabilistic diffusion tractography methods to confirm our observations. Third, the AAL template was used for the network construction. Recent studies have suggested that the node definition by different parcellation scales might result in different properties of brain networks (Wang et al. 2009; Fornito et al. 2010; Zalesky et al. 2010; de Reus and van den Heuvel 2013). Moreover, as some previous studies mentioned (Gong,

Downloaded from https://academic.oup.com/cercor/article/27/1/602/3056183 by guest on 11 October 2020

He, et al. 2009; Li et al. 2009; Wang et al. 2012), fiber bundles may be chosen erroneously if an AAL template contained too many WM voxels that are not truly adjacent to the cortex. However, the gold standard for identifying the nature of the removed WM voxels is still missing. Here, to reduce this false-positive error, we employed a method introduced by Gong, He, et al. (2009), that is, remove WM voxels in the raw AAL template if no cortical voxels existed within their 2 mm cubic neighborhood. In addition, regions on the AAL template differ in size, which may introduce a confounding effect on the link weight of the network nodes (van den Heuvel et al. 2010; Wang et al. 2012). To address this issue, we performed a post hoc analysis on the voxel count difference in the AAL template and found no significant result between patients and controls (data not shown), suggesting an equivalent effect of region size on the network metrics in both groups. Furthermore, although several network edge weighting methods (e.g., streamline density and streamline density with length correction) have been introduced to compensate the region of interest (ROI) size effect (Hagmann et al. 2008; Buchanan et al. 2014), the choice of the most accurate representation of the underlying neurobiological connectivity remains an open question (Jones et al. 2013). The main focus of the current work is to investigate the abnormal hemispheric asymmetry of brain anatomical networks in schizophrenia. We believe that graph theoretical analyses with different resolutions and more accurate edge weighting method in future studies would also be important for better understanding the schizophrenia specific alterations in hemispheric asymmetry. Finally, as our study is one of the first exploratory investigations of abnormal hemispheric asymmetry of structural brain networks in schizophrenia, we did not perform corrections for the multiple comparisons of the global network metrics as well as the correlation coefficients between the hemispheric asymmetry scores and clinical features and mainly focused on the interpretation of the patterns of the findings. We also provided the exact statistical analysis results for the reader's interpretation. Nevertheless, future studies using an independent study sample and hypothesis-driven study design are expected.

In conclusion, graph theoretical analysis of the brain anatomical networks at the "whole-hemisphere" level, as performed in this study, provides the first opportunity to investigate the broader network asymmetries as well as impaired structural connectivity in schizophrenia. We found that beyond a dysconnectivity pattern, there is a reduced hemispheric asymmetry in WM topological properties both globally and regionally in schizophrenia, which are also correlated with clinical features of illness. These findings provide evidence to support the notion that altered hemispheric asymmetry at the level of the connectome may underline abnormal brain function and clinical symptoms observed in schizophrenia and highlight the potential of brain network measures as neural biomarkers for clinical presentation of schizophrenia.

Supplementary Material

Supplementary material can be found at http://www.cercor.oxfordjournals.org/.

Funding

This work was supported by the National Healthcare Group (grant no. NHG 11003 and 12003 awarded to K.S.) and Agency for Science, Technology, Research/Singapore BioImaging Consortium (grant no. ASTAR/SBIC 009/2006 awarded to K.S.). The authors thank the National University of Singapore for supporting the Cognitive Engineering Group at the Singapore Institute for Neurotechnology (SINAPSE) under grant no. R-719-001-102-232.

Notes

The authors are grateful to Mr Renick Lee for his assistance in data preprocessing. The authors thank all patients and controls for their participation. *Conflict of Interest*: None declared.

References

Achard S, Bullmore E. 2007. Efficiency and cost of economical brain functional networks. PLoS Comput Biol. 3:e17.

Achard S, Salvador R, Whitcher B, Suckling J, Bullmore E. 2006. A resilient, low-frequency, small-world human brain functional network with highly connected association cortical hubs. J Neurosci. 26:63–72.

Andreasen NC, Nopoulos P, Magnotta V, Pierson R, Ziebell S, Ho BC. 2011. Progressive brain change in schizophrenia: a prospective longitudinal study of first-episode schizophrenia. Biol Psychiatry. 70:672–679.

Bai F, Shu N, Yuan Y, Shi Y, Yu H, Wu D, Wang J, Xia M, He Y, Zhang Z. 2012. Topologically convergent and divergent structural connectivity patterns between patients with remitted geriatric depression and amnestic mild cognitive impairment. J Neurosci. 32:4307–4318.

Barrick TR, Mackay CE, Prima S, Maes F, Vandermeulen D, Crow TJ, Roberts N. 2005. Automatic analysis of cerebral asymmetry: an exploratory study of the relationship between brain torque and planum temporale asymmetry. NeuroImage. 24:678–691.

Bassett DS, Bullmore ET. 2009. Human brain networks in health and disease. Curr Opin Neurol. 22:340–347.

Bassett DS, Bullmore E, Verchinski BA, Mattay VS, Weinberger DR, Meyer-Lindenberg A. 2008. Hierarchical organization of human cortical networks in health and schizophrenia. J Neurosci. 28:9239–9248.

Bilder RM, Wu H, Bogerts B, Degreef G, Ashtari M, Alvir JM, Snyder PJ, Lieberman JA. 1994. Absence of regional hemispheric volume asymmetries in first-episode schizophrenia. Am J Psychiatry. 151:1437–1447.

Boccaletti S, Latora V, Moreno Y, Chavez M, Hwang DU. 2006. Complex networks: structure and dynamics. Phys Rep. 424:175–308.

Buchanan CR, Pernet CR, Gorgolewski KJ, Storkey AJ, Bastin ME. 2014. Test-retest reliability of structural brain networks from diffusion MRI. NeuroImage. 86:231–243.

Bullmore E, Sporns O. 2009. Complex brain networks: graph theoretical analysis of structural and functional systems. Nat Rev Neurosci. 10:186–198.

Bullmore ET, Frangou S, Murray RM. 1997. The dysplastic net hypothesis: an integration of developmental and dysconnectivity theories of schizophrenia. Schizophr Res. 28:143–156.

Cabeza R. 2002. Hemispheric asymmetry reduction in older adults: the HAROLD model. Psychol Aging. 17:85–100.

Cao Y, Whalen S, Huang J, Berger KL, DeLano MC. 2003. Asymmetry of subinsular anisotropy by in vivo diffusion tensor imaging. Hum Brain Mapp. 20:82–90.

Carletti F, Woolley JB, Bhattacharyya S, Perez-Iglesias R, Fusar Poli P, Valmaggia L, Broome MR, Bramon E, Johns L, Giampietro V, et al. 2012. Alterations in white matter evident before the onset of psychosis. Schizophr Bull. 38:1170–1179.

Downloaded from https://academic.oup.com/cercor/article/27/1/602/3056183 by guest on 11 October 2020

Chan RC, Di X, McAlonan GM, Gong QY. 2011. Brain anatomical abnormalities in high-risk individuals, first-episode, and chronic schizophrenia: an activation likelihood estimation meta-analysis of illness progression. Schizophr Bull. 37: 177–188.

Collinson SL, Mackay CE, James AC, Quested DJ, Phillips T, Roberts N, Crow TJ. 2003. Brain volume, asymmetry and intellectual impairment in relation to sex in early-onset schizophrenia. Br J Psychiatry. 183:114–120.

Collinson SL, Mackay CE, O Jiaqing, James AC, Crow TJ. 2009. Dichotic listening impairments in early onset schizophrenia are associated with reduced left temporal lobe volume. Schizophr Res. 112:24–31.

Crow TJ. 2008. The "big bang" theory of the origin of psychosis and the faculty of language. Schizophr Res. 102:31–52.

Crow TJ, Ball J, Bloom SR, Brown R, Bruton CJ, Colter N, Frith CD, Johnstone EC, Owens DG, Roberts GW. 1989. Schizophrenia as an anomaly of development of cerebral asymmetry. A postmortem study and a proposal concerning the genetic basis of the disease. Arch Gen Psychiatry. 46:1145–1150.

Cui Z, Zhong S, Xu P, He Y, Gong G. 2013. PANDA: a pipeline toolbox for analyzing brain diffusion images. Front Hum Neurosci. 7:42.

Cutting J. 1992. The role of right hemisphere dysfunction in psychiatric disorders. Br J Psychiatry. 160:583–588.

DeLisi LE, Sakuma M, Kushner M, Finer DL, Hoff AL, Crow TJ. 1997. Anomalous cerebral asymmetry and language processing in schizophrenia. Schizophr Bull. 23:255–271.

de Reus MA, van den Heuvel MP. 2013. The parcellation-based connectome: limitations and extensions. NeuroImage. 80:397–404.

Ellison-Wright I, Bullmore E. 2009. Meta-analysis of diffusion tensor imaging studies in schizophrenia. Schizophr Res. 108:3–10.

Falkai P, Bogerts B, Schneider T, Greve B, Pfeiffer U, Pilz K, Gonsiorzcyk C, Majtenyi C, Ovary I. 1995. Disturbed planum temporale asymmetry in schizophrenia. A quantitative postmortem study. Schizophr Res. 14:161–176.

Fitzsimmons J, Kubicki M, Shenton ME. 2013. Review of functional and anatomical brain connectivity findings in schizophrenia. Curr Opin Psychiatry. 26:172–187.

Fornito A, Zalesky A, Bullmore ET. 2010. Network scaling effects in graph analytic studies of human resting-state FMRI data. Front Syst Neurosci. 4:22.

Fornito A, Zalesky A, Pantelis C, Bullmore ET. 2012. Schizophrenia, neuroimaging and connectomics. NeuroImage. 62:2296–2314.

Fried I, Wilson CL, MacDonald KA, Behnke EJ. 1998. Electric current stimulates laughter. Nature. 391:650.

Friston KJ. 1998. The disconnection hypothesis. Schizophr Res. 30:115–125.

Galaburda AM, LeMay M, Kemper TL, Geschwind N. 1978. Right-left asymmetrics in the brain. Science. 199:852–856.

Geschwind N, Levitsky W. 1968. Human brain: left-right asymmetries in temporal speech region. Science. 161:186–187.

Glasser MF, Rilling JK. 2008. DTI tractography of the human brain's language pathways. Cereb Cortex. 18:2471–2482.

Goldberg II, Harel M, Malach R. 2006. When the brain loses its self: prefrontal inactivation during sensorimotor processing. Neuron. 50:329–339.

Gong G, He Y, Concha L, Lebel C, Gross DW, Evans AC, Beaulieu C. 2009. Mapping anatomical connectivity patterns of human cerebral cortex using in vivo diffusion tensor imaging tractography. Cereb Cortex. 19:524–536.

Gong G, Jiang T, Zhu C, Zang Y, Wang F, Xie S, Xiao J, Guo X. 2005. Asymmetry analysis of cingulum based on scale-invariant parameterization by diffusion tensor imaging. Hum Brain Mapp. 24:92–98.

Gong G, Rosa-Neto P, Carbonell F, Chen ZJ, He Y, Evans AC. 2009. Age- and gender-related differences in the cortical anatomical network. J Neurosci. 29:15684–15693.

Good CD, Johnsrude I, Ashburner J, Henson RN, Friston KJ, Frackowiak RS. 2001. Cerebral asymmetry and the effects of sex and handedness on brain structure: a voxel-based morphometric analysis of 465 normal adult human brains. NeuroImage. 14:685–700.

Gotts SJ, Jo HJ, Wallace GL, Saad ZS, Cox RW, Martin A. 2013. Two distinct forms of functional lateralization in the human brain. Proc Natl Acad Sci USA. 110:E3435–E3444.

Griffa A, Baumann PS, Thiran JP, Hagmann P. 2013. Structural connectomics in brain diseases. NeuroImage. 80:515–526.

Hagmann P, Cammoun L, Gigandet X, Meuli R, Honey CJ, Wedeen VJ, Sporns O. 2008. Mapping the structural core of human cerebral cortex. PLoS Biol. 6:e159.

Harrison PJ. 2004. The hippocampus in schizophrenia: a review of the neuropathological evidence and its pathophysiological implications. Psychopharmacology. 174:151–162.

He Y, Evans A. 2010. Graph theoretical modeling of brain connectivity. Curr Opin Neurol. 23:341–350.

Heinrichs RW, Zakzanis KK. 1998. Neurocognitive deficit in schizophrenia: a quantitative review of the evidence. Neuropsychology. 12:426–445.

Herve PY, Crivello F, Perchey G, Mazoyer B, Tzourio-Mazoyer N. 2006. Handedness and cerebral anatomical asymmetries in young adult males. NeuroImage. 29:1066–1079.

Herve PY, Zago L, Petit L, Mazoyer B, Tzourio-Mazoyer N. 2013. Revisiting human hemispheric specialization with neuroimaging. Trends Cogn Sci. 17:69–80.

Highley JR, McDonald B, Walker MA, Esiri MM, Crow TJ. 1999. Schizophrenia and temporal lobe asymmetry. A post-mortem stereological study of tissue volume. Br J Psychiatry. 175:127–134.

Howes OD, Murray RM. 2014. Schizophrenia: an integrated socio-developmental-cognitive model. Lancet. 383:1677–1687.

Iturria-Medina Y, Perez Fernandez A, Morris DM, Canales-Rodriguez EJ, Haroon HA, Garcia Penton L, Augath M, Galan Garcia L, Logothetis N, Parker GJ, et al. 2011. Brain hemispheric structural efficiency and interconnectivity rightward asymmetry in human and nonhuman primates. Cereb Cortex. 21:56–67.

Jalili M, Meuli R, Do KQ, Hasler M, Crow TJ, Knyazeva MG. 2010. Attenuated asymmetry of functional connectivity in schizophrenia: a high-resolution EEG study. Psychophysiology. 47:706–716.

Jenkinson M, Bannister P, Brady M, Smith S. 2002. Improved optimization for the robust and accurate linear registration and motion correction of brain images. NeuroImage. 17:825–841.

Jones DK. 2010. Challenges and limitations of quantifying brain connectivity in vivo with diffusion MRI. Imaging Med. 2:341–355.

Jones DK, Knosche TR, Turner R. 2013. White matter integrity, fiber count, and other fallacies: the do's and don'ts of diffusion MRI. NeuroImage. 73:239–254.

Kanaan R, Barker G, Brammer M, Giampietro V, Shergill S, Woolley J, Picchioni M, Toulopoulou T, McGuire P. 2009. White matter microstructure in schizophrenia: effects of disorder, duration and medication. Br J Psychiatry. 194:236–242.

Kanaan RA, Kim JS, Kaufmann WE, Pearlson GD, Barker GJ, McGuire PK. 2005. Diffusion tensor imaging in schizophrenia. Biol Psychiatry. 58:921–929.

Kay SR, Fiszbein A, Opler LA. 1987. The positive and negative syndrome scale (PANSS) for schizophrenia. Schizophr Bull. 13:261–276.

Downloaded from https://academic.oup.com/cercor/article/27/1/602/3056183 by guest on 11 October 2020

Kubicki M, Alvarado JL, Westin CF, Tate DF, Markant D, Terry DP, Whitford TJ, De Siebenthal J, Bouix S, McCarley RW, et al. 2011. Stochastic tractography study of inferior frontal gyrus anatomical connectivity in schizophrenia. NeuroImage. 55: 1657–1664.

Kubicki M, McCarley R, Westin CF, Park HJ, Maier S, Kikinis R, Jolesz FA, Shenton ME. 2007. A review of diffusion tensor imaging studies in schizophrenia. J Psychiatr Res. 41:15–30.

Kubicki M, Shenton ME. 2014. Diffusion tensor imaging findings and their implications in schizophrenia. Curr Opin Psychiatry. 27:179–184.

Kubicki M, Westin CF, Maier SE, Frumin M, Nestor PG, Salisbury DF, Kikinis R, Jolesz FA, McCarley RW, Shenton ME. 2002. Uncinate fasciculus findings in schizophrenia: a magnetic resonance diffusion tensor imaging study. Am J Psychiatry. 159:813–820.

Kubicki M, Westin CF, Nestor PG, Wible CG, Frumin M, Maier SE, Kikinis R, Jolesz FA, McCarley RW, Shenton ME. 2003. Cingulate fasciculus integrity disruption in schizophrenia: a magnetic resonance diffusion tensor imaging study. Biol Psychiatry. 54:1171–1180.

Kunimatsu N, Aoki S, Kunimatsu A, Yoshida M, Abe O, Yamada H, Masutani Y, Kasai K, Yamasue H, Ohtsu H, et al. 2008. Tract-specific analysis of the superior occipitofrontal fasciculus in schizophrenia. Psychiatry Res. 164:198–205.

Lancaster JL, Kochunov PV, Thompson PM, Toga AW, Fox PT. 2003. Asymmetry of the brain surface from deformation field analysis. Hum Brain Mapp. 19:79–89.

Latora V, Marchiori M. 2001. Efficient behavior of small-world networks. Phys Rev Lett. 87:198701.

Li YH, Liu Y, Li J, Qin W, Li KC, Yu CS, Jiang TZ. 2009. Brain anatomical network and intelligence. PLoS Comput Biol. 5(5): e1000395.

Liu Y, Liang M, Zhou Y, He Y, Hao Y, Song M, Yu C, Liu H, Liu Z, Jiang T. 2008. Disrupted small-world networks in schizophrenia. Brain. 131:945–961.

Luchins DJ, Weinberger DR, Wyatt RJ. 1982. Schizophrenia and cerebral asymmetry detected by computed tomography. Am J Psychiatry. 139:753–757.

Luders E, Narr KL, Thompson PM, Rex DE, Jancke L, Toga AW. 2006. Hemispheric asymmetries in cortical thickness. Cereb Cortex. 16:1232–1238.

McCarley RW, Wible CG, Frumin M, Hirayasu Y, Levitt JJ, Fischer IA, Shenton ME. 1999. MRI anatomy of schizophrenia. Biol Psychiatry. 45:1099–1119.

McGlashan TH, Hoffman RE. 2000. Schizophrenia as a disorder of developmentally reduced synaptic connectivity. Arch Gen Psychiatry. 57:637–648.

Mesholam-Gately RI, Giuliano AJ, Goff KP, Faraone SV, Seidman LJ. 2009. Neurocognition in first-episode schizophrenia: a meta-analytic review. Neuropsychology. 23:315–336.

Mesulam MM. 1998. From sensation to cognition. Brain. 121(Pt 6):1013–1052.

Micheloyannis S, Pachou E, Stam CJ, Breakspear M, Bitsios P, Vourkas M, Erimaki S, Zervakis M. 2006. Small-world networks and disturbed functional connectivity in schizophrenia. Schizophr Res. 87:60–66.

Mitchell RL, Crow TJ. 2005. Right hemisphere language functions and schizophrenia: the forgotten hemisphere? Brain. 128:963–978.

Miyata J, Sasamoto A, Koelkebeck K, Hirao K, Ueda K, Kawada R, Fujimoto S, Tanaka Y, Kubota M, Fukuyama H, et al. 2012. Abnormal asymmetry of white matter integrity in schizophrenia revealed by voxelwise diffusion tensor imaging. Hum Brain Mapp. 33:1741–1749.

Mori S, Crain BJ, Chacko VP, van Zijl PC. 1999. Three-dimensional tracking of axonal projections in the brain by magnetic resonance imaging. Ann Neurol. 45:265–269.

Mueller S, Wang D, Pan R, Holt DJ, Liu H. 2015. Abnormalities in hemispheric specialization of caudate nucleus connectivity in schizophrenia. JAMA Psychiatry. 72:552–560.

Navari S, Dazzan P. 2009. Do antipsychotic drugs affect brain structure? A systematic and critical review of MRI findings. Psychol Med. 39:1763–1777.

Oertel-Knochel V, Linden DE. 2011. Cerebral asymmetry in schizophrenia. Neuroscientist. 17:456–467.

Ottet MC, Schaer M, Debbane M, Cammoun L, Thiran JP, Eliez S. 2013. Graph theory reveals dysconnected hubs in 22q11DS and altered nodal efficiency in patients with hallucinations. Front Hum Neurosci. 7:402.

Park HJ, Westin CF, Kubicki M, Maier SE, Niznikiewicz M, Baer A, Frumin M, Kikinis R, Jolesz FA, McCarley RW, et al. 2004. White matter hemisphere asymmetries in healthy subjects and in schizophrenia: a diffusion tensor MRI study. NeuroImage. 23:213–223.

Parker GJ, Luzzi S, Alexander DC, Wheeler-Kingshott CA, Ciccarelli O, Lambon Ralph MA. 2005. Lateralization of ventral and dorsal auditory-language pathways in the human brain. NeuroImage. 24:656–666.

Pettersson-Yeo W, Allen P, Benetti S, McGuire P, Mechelli A. 2011. Dysconnectivity in schizophrenia: where are we now? Neurosci Biobehav Rev. 35:1110–1124.

Ratnarajah N, Rifkin-Graboi A, Fortier MV, Chong YS, Kwek K, Saw SM, Godfrey KM, Gluckman PD, Meaney MJ, Qiu A. 2013. Structural connectivity asymmetry in the neonatal brain. NeuroImage. 75:187–194.

Ribolsi M, Daskalakis ZJ, Siracusano A, Koch G. 2014. Abnormal asymmetry of brain connectivity in schizophrenia. Front Hum Neurosci. 8:1010.

Ribolsi M, Koch G, Magni V, Di Lorenzo G, Rubino IA, Siracusano A, Centonze D. 2009. Abnormal brain lateralization and connectivity in schizophrenia. Rev Neurosci. 20:61–70.

Rubinov M, Bullmore E. 2013. Schizophrenia and abnormal brain network hubs. Dialogues Clin Neurosci. 15:339–349.

Rubinov M, Knock SA, Stam CJ, Micheloyannis S, Harris AW, Williams LM, Breakspear M. 2009. Small-world properties of nonlinear brain activity in schizophrenia. Hum Brain Mapp. 30:403–416.

Rubinov M, Sporns O. 2010. Complex network measures of brain connectivity: uses and interpretations. NeuroImage. 52:1059–1069.

Schachter SC, Ransil BJ, Geschwind N. 1987. Associations of handedness with hair color and learning disabilities. Neuropsychologia. 25:269–276.

Shapleske J, Rossell SL, Chitnis XA, Suckling J, Simmons A, Bullmore ET, Woodruff PW, David AS. 2002. A computational morphometric MRI study of schizophrenia: effects of hallucinations. Cereb Cortex. 12:1331–1341.

Shenton ME, Dickey CC, Frumin M, McCarley RW. 2001. A review of MRI findings in schizophrenia. Schizophr Res. 49:1–52.

Shenton ME, Kikinis R, Jolesz FA, Pollak SD, LeMay M, Wible CG, Hokama H, Martin J, Metcalf D, Coleman M, et al. 1992. Abnormalities of the left temporal lobe and thought disorder in schizophrenia. A quantitative magnetic resonance imaging study. N Engl J Med. 327:604–612.

Shu N, Liu Y, Li K, Duan Y, Wang J, Yu C, Dong H, Ye J, He Y. 2011. Diffusion tensor tractography reveals disrupted topological efficiency in white matter structural networks in multiple sclerosis. Cereb Cortex. 21:2565–2577.

Smith SM, Jenkinson M, Woolrich MW, Beckmann CF, Behrens TE, Johansen-Berg H, Bannister PR, De Luca M, Drobnjak I,

Downloaded from https://academic.oup.com/cercor/article/27/1/602/3056183 by guest on 11 October 2020

Flitney DE, et al. 2004. Advances in functional and structural MR image analysis and implementation as FSL. NeuroImage. 23(Suppl 1):S208–S219.
Sommer I, Ramsey N, Kahn R, Aleman A, Bouma A. 2001. Handedness, language lateralisation and anatomical asymmetry in schizophrenia: meta-analysis. Br J Psychiatry. 178:344–351.
Song JW, Mitchell PD, Kolasinski J, Ellen Grant P, Galaburda AM, Takahashi E. 2014. Asymmetry of white matter pathways in developing human brains. Cereb Cortex. 25(9):2883–2893.
Sporns O. 2011. The human connectome: a complex network. Ann N Y Acad Sci. 1224:109–125.
Stam CJ. 2014. Modern network science of neurological disorders. Nat Rev Neurosci. 15:683–695.
Stephan KE, Baldeweg T, Friston KJ. 2006. Synaptic plasticity and dysconnection in schizophrenia. Biol Psychiatry. 59:929–939.
Stephan KE, Friston KJ, Frith CD. 2009. Dysconnection in schizophrenia: from abnormal synaptic plasticity to failures of self-monitoring. Schizophr Bull. 35:509–527.
Takao H, Abe O, Yamasue H, Aoki S, Kasai K, Ohtomo K. 2010. Cerebral asymmetry in patients with schizophrenia: a voxel-based morphometry (VBM) and diffusion tensor imaging (DTI) study. J Magn Reson Imaging. 31:221–226.
Takao H, Abe O, Yamasue H, Aoki S, Sasaki H, Kasai K, Yoshioka N, Ohtomo K. 2011. Gray and white matter asymmetries in healthy individuals aged 21–29 years: a voxel-based morphometry and diffusion tensor imaging study. Hum Brain Mapp. 32:1762–1773.
Takao H, Hayashi N, Ohtomo K. 2011. White matter asymmetry in healthy individuals: a diffusion tensor imaging study using tract-based spatial statistics. Neuroscience. 193:291–299.
Tian L, Wang J, Yan C, He Y. 2011. Hemisphere- and gender-related differences in small-world brain networks: a resting-state functional MRI study. NeuroImage. 54:191–202.
Toga AW, Thompson PM. 2003. Mapping brain asymmetry. Nat Rev Neurosci. 4:37–48.
Torrey EF. 2007. Schizophrenia and the inferior parietal lobule. Schizophr Res. 97:215–225.
Tzourio-Mazoyer N, Landeau B, Papathanassiou D, Crivello F, Etard O, Delcroix N, Mazoyer B, Joliot M. 2002. Automated anatomical labeling of activations in SPM using a macroscopic anatomical parcellation of the MNI MRI single-subject brain. NeuroImage. 15:273–289.
Uhlhaas PJ. 2013. Dysconnectivity, large-scale networks and neuronal dynamics in schizophrenia. Curr Opin Neurobiol. 23:283–290.
van den Heuvel MP, Fornito A. 2014. Brain networks in schizophrenia. Neuropsychol Rev. 24:32–48.
van den Heuvel MP, Mandl RC, Stam CJ, Kahn RS, Hulshoff Pol HE. 2010. Aberrant frontal and temporal complex network structure in schizophrenia: a graph theoretical analysis. J Neurosci. 30:15915–15926.
van den Heuvel MP, Sporns O, Collin G, Scheewe T, Mandl RC, Cahn W, Goni J, Hulshoff Pol HE, Kahn RS. 2013. Abnormal rich club organization and functional brain dynamics in schizophrenia. JAMA Psychiatry. 70:783–792.
Vernooij MW, Smits M, Wielopolski PA, Houston GC, Krestin GP, van der Lugt A. 2007. Fiber density asymmetry of the arcuate fasciculus in relation to functional hemispheric language lateralization in both right- and left-handed healthy subjects: a combined fMRI and DTI study. NeuroImage. 35:1064–1076.
Wang F, Sun Z, Cui L, Du X, Wang X, Zhang H, Cong Z, Hong N, Zhang D. 2004. Anterior cingulum abnormalities in male patients with schizophrenia determined through diffusion tensor imaging. Am J Psychiatry. 161:573–575.
Wang J, Wang L, Zang Y, Yang H, Tang H, Gong Q, Chen Z, Zhu C, He Y. 2009. Parcellation-dependent small-world brain functional networks: a resting-state fMRI study. Hum Brain Mapp. 30:1511–1523.
Wang L, Metzak PD, Honer WG, Woodward TS. 2010. Impaired efficiency of functional networks underlying episodic memory-for-context in schizophrenia. J Neurosci. 30:13171–13179.
Wang Q, Su TP, Zhou Y, Chou KH, Chen IY, Jiang T, Lin CP. 2012. Anatomical insights into disrupted small-world networks in schizophrenia. NeuroImage. 59:1085–1093.
Wang R, Benner T, Sorensen AG, Wedeen VJ. 2007. Diffusion toolkit: a software package for diffusion imaging data processing and tractography. Proc Intl Soc Mag Reson Med. 15:3720.
Watkins KE, Paus T, Lerch JP, Zijdenbos A, Collins DL, Neelin P, Taylor J, Worsley KJ, Evans AC. 2001. Structural asymmetries in the human brain: a voxel-based statistical analysis of 142 MRI scans. Cereb Cortex. 11:868–877.
Watts DJ, Strogatz SH. 1998. Collective dynamics of "small-world" networks. Nature. 393:440–442.
Wheeler AL, Voineskos AN. 2014. A review of structural neuroimaging in schizophrenia: from connectivity to connectomics. Front Hum Neurosci. 8:653.
Wu K, Taki Y, Sato K, Kinomura S, Goto R, Okada K, Kawashima R, He Y, Evans AC, Fukuda H. 2012. Age-related changes in topological organization of structural brain networks in healthy individuals. Hum Brain Mapp. 33:552–568.
Xia M, Wang J, He Y. 2013. BrainNet Viewer: a network visualization tool for human brain connectomics. PLoS ONE. 8:e68910.
Yao L, Lui S, Liao Y, Dua MY, Hu N, Thomas JA, Gong QY. 2013. White matter deficits in first episode schizophrenia: an activation likelihood estimation meta-analysis. Prog Neuropsychopharmacol Biol Psychiatry. 45:100–106.
Zalesky A, Fornito A, Harding IH, Cocchi L, Yucel M, Pantelis C, Bullmore ET. 2010. Whole-brain anatomical networks: does the choice of nodes matter? NeuroImage. 50:970–983.
Zalesky A, Fornito A, Seal ML, Cocchi L, Westin CF, Bullmore ET, Egan GF, Pantelis C. 2011. Disrupted axonal fiber connectivity in schizophrenia. Biol Psychiatry. 69:80–89.
Zhang R, Wei Q, Kang Z, Zalesky A, Li M, Xu Y, Li L, Wang J, Zheng L, Wang B, et al. 2015. Disrupted brain anatomical connectivity in medication-naive patients with first-episode schizophrenia. Brain Struct Funct. 220:1145–1159.
Zhang Y, Lin L, Lin CP, Zhou Y, Chou KH, Lo CY, Su TP, Jiang T. 2012. Abnormal topological organization of structural brain networks in schizophrenia. Schizophr Res. 141:109–118.

Downloaded from https://academic.oup.com/cercor/article/27/1/602/3056183 by guest on 11 October 2020